Surface Science 603 (2009) 2255–2262

Contents lists available at ScienceDirect

Surface Science

journal homepage: www.elsevier.com/locate/susc

STM and LEED observations of a c(2 × 2) Ge overlayer on Pt(1 0 0)

Taketoshi Matsumoto [1], Matthias Batzill [2], Bruce E. Koel *

Department of Chemistry and Center for Advanced Materials and Nanotechnology (CAMN), Lehigh University, 6 E. Packer Ave., Bethlehem, PA 18015-3172, United States

ARTICLE INFO

Article history:
Received 27 November 2008
Accepted for publication 20 April 2009
Available online 3 May 2009

Keywords:
Germanium
Platinum
Alloy
Low energy electron diffraction
Scanning tunneling microscopy

ABSTRACT

We have investigated surface structures formed by deposition of 0.2 and 0.5-ML Ge on Pt(1 0 0) by using scanning tunneling microscopy (STM) and low electron energy diffraction (LEED). In addition, their temperature dependence and reactivity to CO have been studied. We observed the formation of disordered domains for Ge adatom coverages below 0.25-ML and complete c(2 × 2) structures at 0.25 to 0.5-ML Ge after annealing at 600–1200 K. Deposition of 0.2-ML Ge on a clean, hexagonally reconstructed (5 × 20)-Pt(1 0 0) substrate at 400 K lifts the reconstruction and ejects excess Pt atoms from the first layer into the adlayer. After annealing this surface to 600 K, the deposited Ge formed Ge adatoms on flat terraces and on round Pt adislands with incomplete c(2 × 2) structures, in addition to the presence of clean (1 × 1)-Pt(1 0 0) domains that were several nanometers across. Some domains of the unreconstructed (5 × 20)-Pt(1 0 0) surface still remained. After the deposition of 0.5-ML Ge and annealing at 600 K, disordered Ge domains disappeared and a c(2 × 2) Ge overlayer was produced all over the surface. Square terraces with square domains of the clean (1 × 1)-Pt(1 0 0) surface extended for nanometers. Annealing this surface to 900 K produced disordered Ge domains, and this was associated with an increase in Ge vacancies. When surfaces with 0.2-ML Ge were heated to 900 or 1200 K, or when a surface with 0.5-ML Ge was heated to 1200 K, larger domains of (5 × 20)-Pt(1 0 0) were formed with the agglomeration of disordered Ge adatoms. Pt clusters were observed in the Ge domains, and we consider these to be composed of those excess Pt atoms formed by lifting the reconstruction of the (5 × 20)-Pt(1 0 0) surface upon Ge agglomeration during cooling. A paper published elsewhere [T. Matsumoto, C. Ho, M. Batzill, B.E. Koel, Physical Review B, submitted for publication.] describes Na^+-ion scattering spectroscopy (Na^+-ISS) and X-ray photoelectron diffraction (XPD) experiments that distinguish between Ge present in an overlayer from incorporation into the top Pt layer to form a surface alloy for the surface structures reported here. Furthermore, these investigations revealed that disordered Ge adatoms observed herein might be associated with incomplete c(2 × 2) structures. Therefore, our observations of the formation of complete and incomplete domains of c(2 × 2) Ge adatoms indicate that interactions between Ge adatoms are repulsive at nearest neighbor distances and attractive at second-nearest neighbor distances. Regarding the reactivity of these surfaces, CO does not chemisorb on a Pt(1 0 0) surface with a c(2 × 2)-Ge *overlayer* and no measurable CO uptake was observed under UHV conditions at 220 K.

1. Introduction

Bimetallic Pt–Ge interfaces and surfaces of Pt–Ge intermetallic compounds are of interest for research and applications in a variety of areas, including electronic devices and detectors [1,2], Pt-based heterogeneous catalysts [3–6], and electrocatalysts for fuel cells [7,8]. In particular, for supported catalysts, the addition of Ge to Pt-loaded HZSM-5 improved the selectivity of butane dehydrogenation to aromatic hydrocarbons [3]. Also, Pt–Ge intermetallic compounds gave high selectivity for the partial hydrogenation of 1,3-butadiene [4]. The selective hydrogenation of carvone ($C_{10}H_{14}O$) to unsaturated ketones was enhanced by adding Ge to Pt/Al_2O_3 catalysts [5]. Resistance to both coking and sulfur deactivation in conventional naphtha reforming processes was produced by Ge addition to Pt/Al_2O_3 catalysts [6]. In fuel cell applications, Ge islands on Pt electrodes accelerated oxidation of CO, HCOOH, HCHO and CH_3OH [7,8], but prohibited hydrogen adsorption [7].

Analogous to the extensive studies of silicides, Pt–Ge compound surfaces and other bimetallic Pt–Ge interfaces have been characterized. Thermodynamic investigations have been reported for formation of surface alloys on Pt/Ge(1 0 0) [1] and Pt/Ge(1 1 1) [2], and for Pt–Ge bulk alloys [9,10]. The composition ranges from Pt_3Ge to $PtGe_2$. Interestingly, deposition of Ge on a Pt(1 1 1) surface forms a highly dispersed $(\sqrt{19} \times \sqrt{19})$R23.4°-$Pt_{18}Ge$ [11] and

* Corresponding author. Tel.: +1 610 758 5650; fax: +1 610 758 6536.
E-mail address: brk205@lehigh.edu (B.E. Koel).
[1] Present address: Institute of Scientific and Industrial Research, Osaka University, Osaka 567-0047, Japan.
[2] Present address: Department of Physics, University of South Florida, Tampa, FL 33620-5700, United States.

0039-6028/$ - see front matter © 2009 Elsevier B.V. All rights reserved.
doi:10.1016/j.susc.2009.04.028

(5×5)-$Pt_{24}Ge$ [12] surface alloy. The former structure was prepared by deposition of 1-ML Ge and annealing at 1000 K and the latter structure by deposition of 2-ML Ge and annealing at 1300 K. To date, there has been no clear explanation for the reason why such a dilute surface alloy is formed. The presence of even this small amount of alloyed Ge strongly altered the Pt(1 1 1) surface reactivity. Surface Ge atoms block CO adsorption sites, lower the desorption temperature of CO and NO adsorbing at Pt sites, and inhibit CO photodesorption. This has been attributed to *p–d* hybridization between Ge and Pt atoms [11–15].

The topmost layer of a Pt(1 0 0) crystal reconstructs to pseudo-hexagonal structures that exhibit Moiré patterns [16–18]. The (5×20)-Pt(1 0 0) surface reduces the total surface energy by 17% *via* packing ~20% more Pt atoms into the topmost layer compared to that of the (1×1)-(1 0 0) surface [16–18]. Changes in this surface structure have been observed during metal deposition and film growth of Sm [19], Au [20] and Ag [21] on Pt(1 0 0). Deposition removes this reconstruction and ejects Pt into the adlayer comprised of elongated islands. We observed previously that Ag evaporation formed long adislands with straight step edges and attributed this to the anisotropic stability of the hex-reconstruction, with the row pattern of the reconstruction acting as a template for island growth [21].

In this report, we characterize and discuss surface structures formed by deposition of Ge on a Pt(1 0 0) crystal substrate. These surfaces were investigated by scanning tunneling microscopy (STM) and low electron energy diffraction (LEED). The temperature and coverage dependence of these structures was also investigated and these are discussed. In addition, we used CO to probe some aspects of the chemical properties of the Ge/Pt(1 0 0) surface. A separate paper [22] extends this work to the assignment of surface and subsurface structures by alkali ion scattering spectroscopy (ALISS), X-ray photoelectron spectroscopy (XPS), and X-ray photoelectron diffraction (XPD).

2. Experimental methods

Experiments were carried out in an ultrahigh vacuum (UHV) chamber that has been described previously [23]. Clean Pt(1 0 0) crystal surfaces were prepared by many cycles of Ar^+-ion sputtering, annealing in an O_2 partial pressure of 2×10^{-7} torr at 1000 K, and flashing to 1200 K in vacuum. The quality of the clean surfaces was checked by STM and LEED.

Germanium was evaporated by resistively heating a W boat that contained high-purity Ge ingots. Following outgassing for 10 min prior to deposition on the Pt(1 0 0) substrate, XPS showed that a clean Ge film could be produced with high reproducibility. The Ge coverage was calculated from the Ge-deposition time, because Ge was not removed from the surface by annealing at 600 K (XPS and XPD results reported elsewhere [22] show that no Ge dissolution occurred under these conditions). A Ge coverage of 0.5-ML was assigned to the appearance of the sharpest spots in the $c(2 \times 2)$ LEED pattern after annealing at 600 K. Here, 1-ML is defined as the surface atom density of the unreconstructed, ideally terminated Pt(1 0 0) surface.

All of the STM images that are reported were acquired in the constant current mode with the substrate at room temperature.

3. Results

3.1. STM observations

3.1.1. 0.2-ML Ge/Pt(1 0 0) surface

STM topographs were acquired after 0.2-ML Ge was deposited on Pt(1 0 0) at 400 K. LEED still showed a (5×20) pattern from this surface, similar to that for the clean (5×20)-Pt(1 0 0) substrate prior to deposition. The STM image of Fig. 1a shows bright dots in disordered rows along the $[0\,1\,\bar{1}]$ direction in the domain labeled ***A***. The amplified view presented in Fig. 1b reveals that the apparent corrugations of the brighter domains ***A*** are 0.12–0.23 nm, compared to the top of the (5×20)-Pt(100) surface labeled ***B***. These corrugations correspond to the single-step height of Pt(1 0 0) (0.20 nm) and Ge overlayers (0.16–0.13 nm) as discussed later. This indicates that area ***A*** might consist of a mixture of Pt and Ge atoms. The characteristic Moiré pattern of the (5×20)-Pt(1 0 0) surface was observed in domain ***B***.

After this surface was annealed at 600 K, we observed a faint (1×1) LEED pattern. Four types of domains were found on this surface by STM, as shown in Fig. 2a: bright circular disordered islands ***A*** with diameters on the order of 20 nm; dark domains ***B***

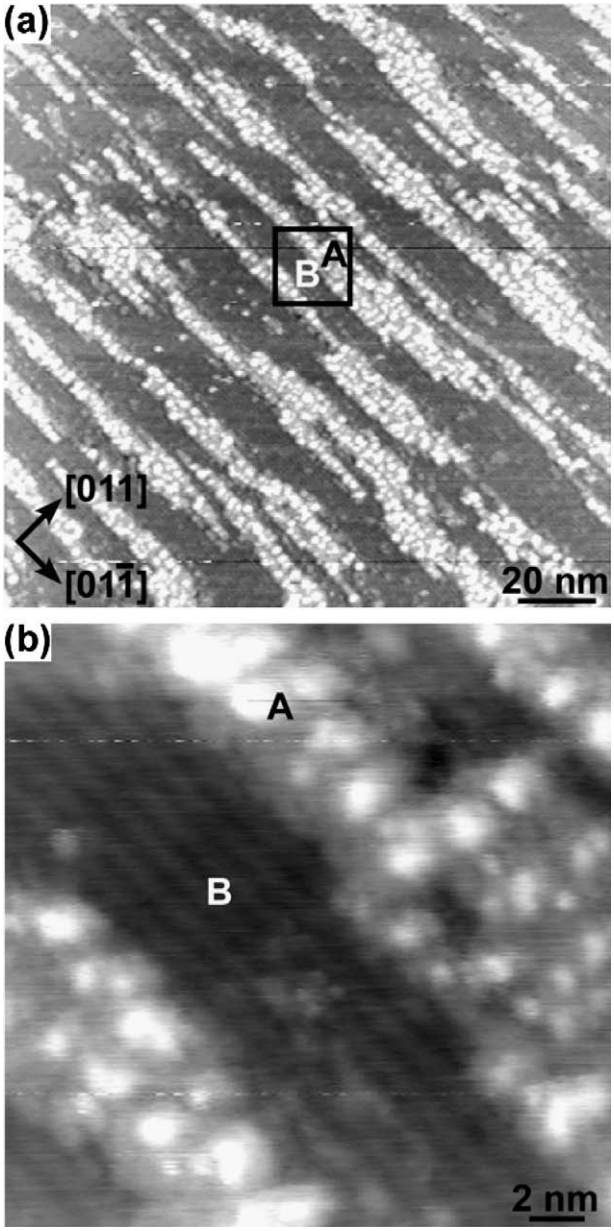

Fig. 1. STM topographs after deposition of 0.2-ML Ge on Pt(1 0 0) at 400 K. (a) Large-area scan. Domains ***A*** are assigned to clusters comprised of intermixed Pt and Ge adatoms and ***B*** are assigned to clean (5×20)-Pt(1 0 0) regions. (b) Amplified view of the area highlighted by the square in (a). $V_s = 0.14$ V, $I_t = 0.16$ nA in both images.

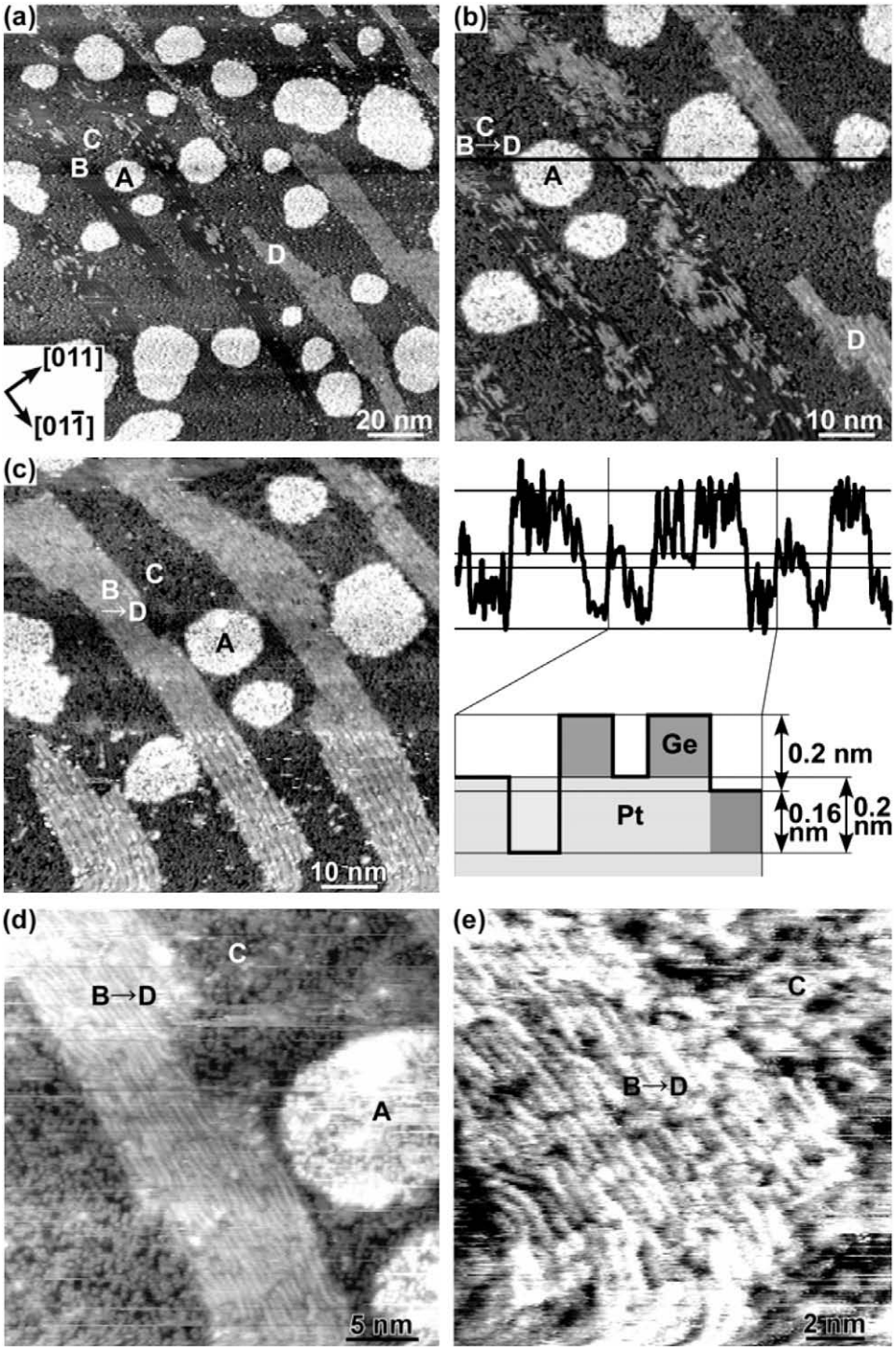

Fig. 2. STM topographs of 0.2-ML Ge/Pt(1 0 0) after annealing at 600 K. Symbols ***A***–***D*** label different domains and are superimposed on the images at the same surface positions in each image. (a) Large-area scan (V_s = 0.12 V, I_t = 0.26 nA). (b) Second scan of the area shown in (a). A cross section along the straight line superimposed on the image is given below the topograph. (c) Third scan of the area shown in (a). (d) Magnified view of domains ***A***–***C***. (e) Magnified view of domains ***B*** (or ***D***) and ***C*** (V_s = 0.11 V, I_t = 0.26 nA). V_s = 0.12 V, I_t = 0.24 nA in images (b), (c) and (d).

exhibiting the (5 × 20)-Pt ordered row structure; dark disordered terraces ***C***; and bright domains ***D*** with partially ordered row structures. Fig. 2b and c show STM images *of the same place* during the second and third subsequent scans, respectively. These images demonstrate that ***B*** domains were unstable and changed to ***D*** domains with increasing number of scans. The cross section along the straight line in Fig. 2b is shown just below the image in (b), and four height-levels can be identified. Domain ***B***, assigned to (5 × 20)-Pt(1 0 0) regions from amplified views, is at the lowest level. Domain ***C***, the second lowest level, is 0.16 nm higher than the lowest level. This region is assigned to disordered Ge overlayers and is discussed further elsewhere [22]. The height difference between the topmost level and domain ***C*** was 0.2 nm, and this corresponds to the single-step height on Pt(1 0 0). This means that the bright islands ***A*** are likely to be Ge overlayers that are located on Pt adislands. The second-highest levels were observed in pits of

the Ge-covered Pt islands ***A*** and in domains ***D***. This level is 0.20 nm higher than the (5 × 20)-Pt(1 0 0) substrate ***B***, indicating that ***D*** domains are due to Pt clusters. Disordered single atoms appearing as bright dots were observed in domains ***A*** and ***C*** shown in Fig. 2d by amplifying the scan of the area shown in Fig. 2c. Fourier transform of the domains ***A*** and ***C*** did not give sharp spots. The Ge atoms in the domains ***A*** and ***C*** are considered to be located mostly on the Pt substrate with a (1 × 1) structure because the height of Ge adatoms are uniform in the same domains in Fig. 2b and Pt adislands (***A***) are found over 20% of the area of the domains ***A*** and ***C***. A domain ***D*** shows continuous bright lines with a length greater than 4 nm, and is assignable to a mixture of the (2 × 1), (3 × 1), (2 × 2) and (3 × 2) structures with Pt atom vacancies from Fig. 2e. The substrate of the domain ***D*** is considered to be mostly (1 × 1) because the row directions were mostly [0 1 $\bar{1}$]. The density of the Pt atoms can be estimated at ~0.2. The Pt adatoms in domain ***D*** are considered to be lifted from the (5 × 20) reconstructed layer with reconstruction to the (1 × 1) structure upon scanning as described by the density of Pt atoms. Domains ***A*** and ***C*** cover 75% of the area of this surface that was formed by depositing 0.2-ML Ge, suggesting that the density of Ge atoms in the region of Ge overlayers is 0.27 (=0.2/0.75), which is about one-half of that for the c(2 × 2)-Ge overlayer shown in the next section.

Annealing the 0.2-ML Ge/Pt(1 0 0) surface at 900 K caused all of the round Pt adislands covered by Ge adatoms to disappear. Weak

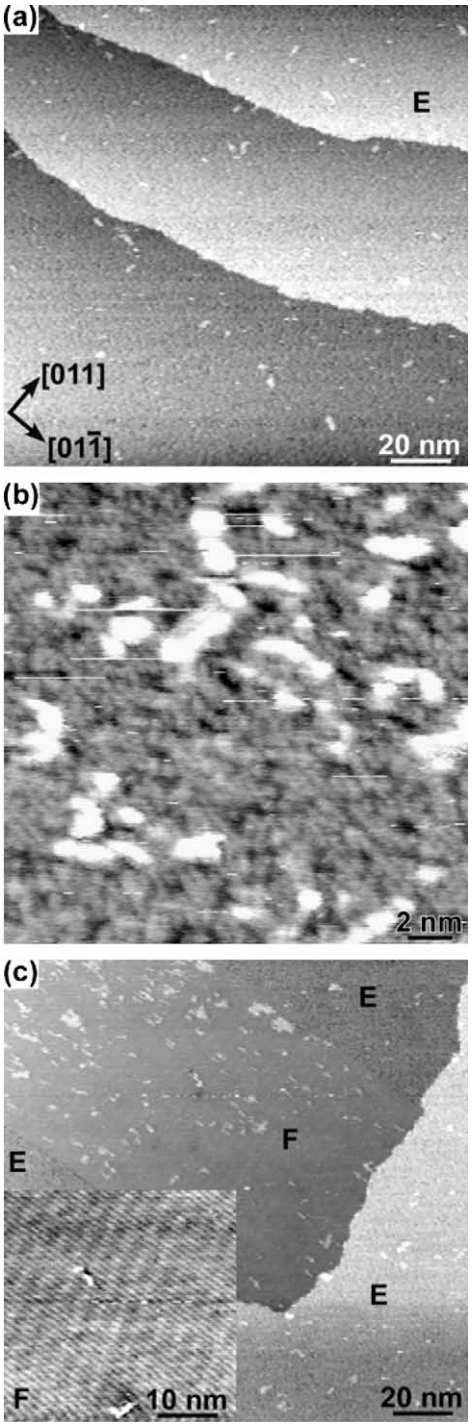

Fig. 3. STM topographs of 0.2-ML Ge/Pt(1 0 0) after annealing at 900 K. (a) Typical large-area scan showing extensive regions labeled as domain ***E*** (V_s = 0.11 V, I_t = 0.16 nA). (b) Amplified view of a terrace in (a) (V_s = 0.11 V, I_t = 0.2 nA). (c) Mixture of Ge-covered and bare Pt(1 0 0) domains. Domains ***E*** and ***F*** are assigned to a Ge overlayer and the clean (5 × 20)-Pt(1 0 0) surface, respectively. The insert gives an amplified view of a (5 × 20)-Pt(1 0 0) domain ***F***. V_s = 0.1 V, I_t = 014 nA in (c) and the insert.

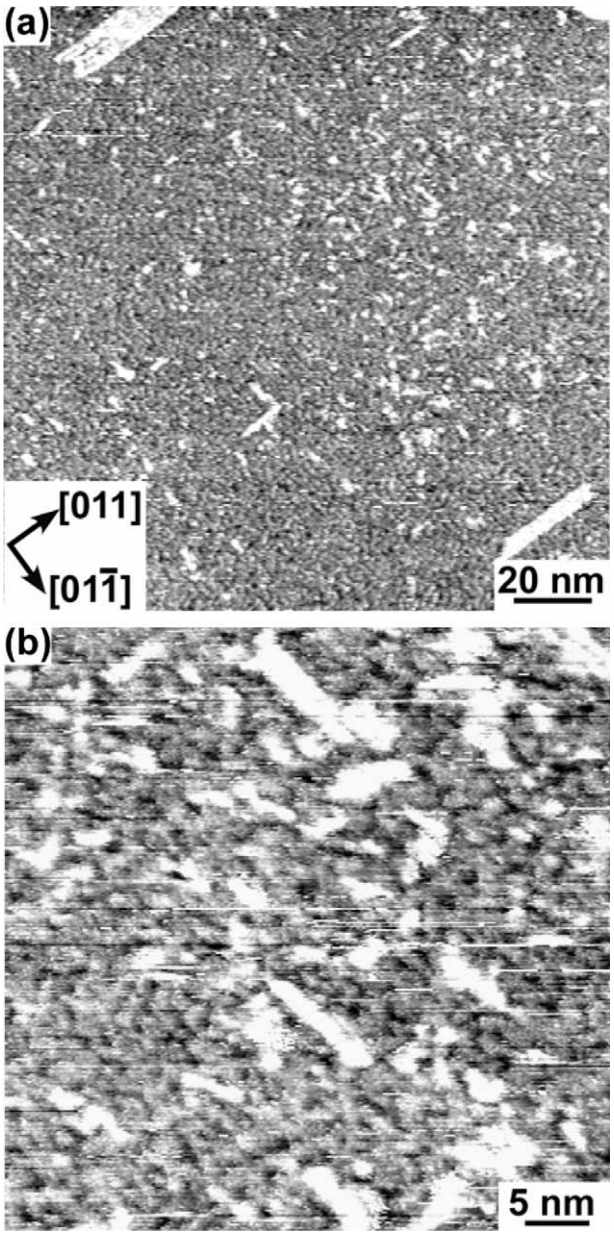

Fig. 4. STM topographs of 0.2-ML Ge/Pt(1 0 0) after annealing at 1200 K. (a) Large-area scan (V_s = 0.1 V, I_t = 0.57 nA). (b) Amplified view of (a) (V_s = 0.1 V, I_t = 0.23 nA).

(5 × 20) LEED spots were observed from this surface. Fig. 3a shows terraces (***E***) that were commonly 100 nm wide, similar in size as those for the original clean Pt(1 0 0) surface. An amplified view of the surface shown in Fig. 3b reveals disordered bright Ge dots, with an apparent height of 0.12 nm from the pits. Some brighter clusters were 0.24–0.33 nm high referenced to the pits. These were found at a density of 0.16, and might be Pt adislands and/or Ge-covered Pt adislands. The magnified images presented in Fig. 3c highlight that the surface also contained (5 × 20)-Pt(1 0 0) domains labeled as ***F***.

No significant change occurred when the annealing temperature was increased to 1200 K. The same LEED pattern was observed, with the same quality. STM images from this surface are shown in Fig. 4. There are no significant differences observed between these images and those presented in Fig. 3. The density of brighter clusters in disordered Ge domains was 0.18.

3.1.2. 0.5-ML Ge/Pt(1 0 0) surface

Depositing 0.5-ML Ge on the Pt(1 0 0) substrate formed a surface that displayed the sharpest c(2 × 2) LEED spots after annealing at 600 K. STM images of this surface showed terraces composed of many smaller square terraces with widths of 10–50 nm, as can be seen in Fig. 5a. Most step edges were directed along [0 0 1] and equivalent azimuths, which is along the close-packed directions of Ge atoms in the c(2 × 2) structure. An amplified view, as given in Fig. 5b, shows homogeneous, ordered bright dots in these terraces, but with some pits. Fig. 5c provides an STM image of a terrace at atomic resolution. The superimposed square indicates the nonprimitive unit cell of the c(2 × 2) structure. The bright spots are assigned to single Ge atoms of a Ge overlayer [22]. A cross section of this surface along the straight line superimposed on Fig. 5d is provided immediately below the image. The height of a single step of terraces was 0.2 nm. The depth of pits (***G***) or line vacancies of Ge along the [0 1 0] direction (***H***) was 0.13 nm from the tops of the terraces. The c(2 × 2) bright dots were observed homogeneously all over the surface except for the small pits (***G***) and line vacancies (***H***).

Annealing this surface at 900 K caused a decrease in the sharpness of the c(2 × 2) spots in the LEED pattern compared to that from the previous surface. XPS was used to determine that the Ge coverage was 0.25-ML [22]. STM images of this surface, as seen in Fig. 6a, showed larger, 30–50-nm wide bright terraces ***I***, with the largest terraces more than 100-nm wide. Dark terraces ***J*** have an apparent height of 0.2-nm lower than the terrace ***I***, and this indicates that they are one atomic layer lower at the surface. Terrace ***I*** contains two kinds of pits denoted as ***K*** and ***L***. Pits ***K*** were observed at the same height as the dark terraces ***J***. Cracks ***M*** were also observed within the terraces. In addition, we observed several islands ***N*** with a height 0.2–0.36-nm higher than the terrace ***I***. The amplified view given in Fig. 6b confirmed the assignment of pits ***L*** on terraces ***I***. The superimposed black square indicates the nonprimitive c(2 × 2) unit cell, and the ordered bright dots in this structure due to Ge adatoms are visible in the terrace. The apparent height difference between domains ***L*** and ***I*** was 0.13 nm, corresponding to the thickness of a single Ge layer. Therefore, domains ***L*** are assignable to regions of Ge vacancies.

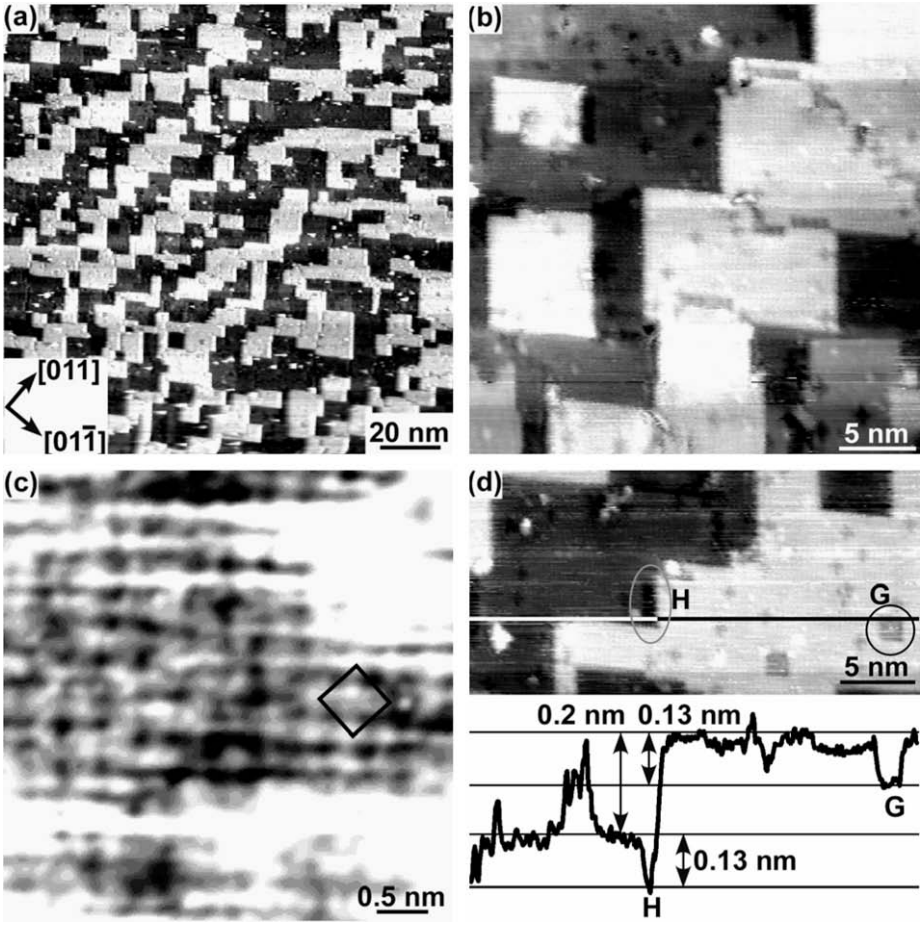

Fig. 5. STM topographs of 0.5-ML Ge/Pt(1 0 0) after annealing at 600 K. (a) Large-area scan (V_s = −0.1 V, I_t = 0.26 nA). (b) Amplified view of (a). (c) Image with atomic resolution. The superimposed square indicates the nonprimitive unit cell of the c(2 × 2) structure. (d) Cross section along the straight line superimposed on the STM image. Domains ***G*** are pits and ***H*** reveals a line-shaped vacancy of Ge. V_s = −0.1 V, I_t = 0.29 nA for images in (b), (c) and (d).

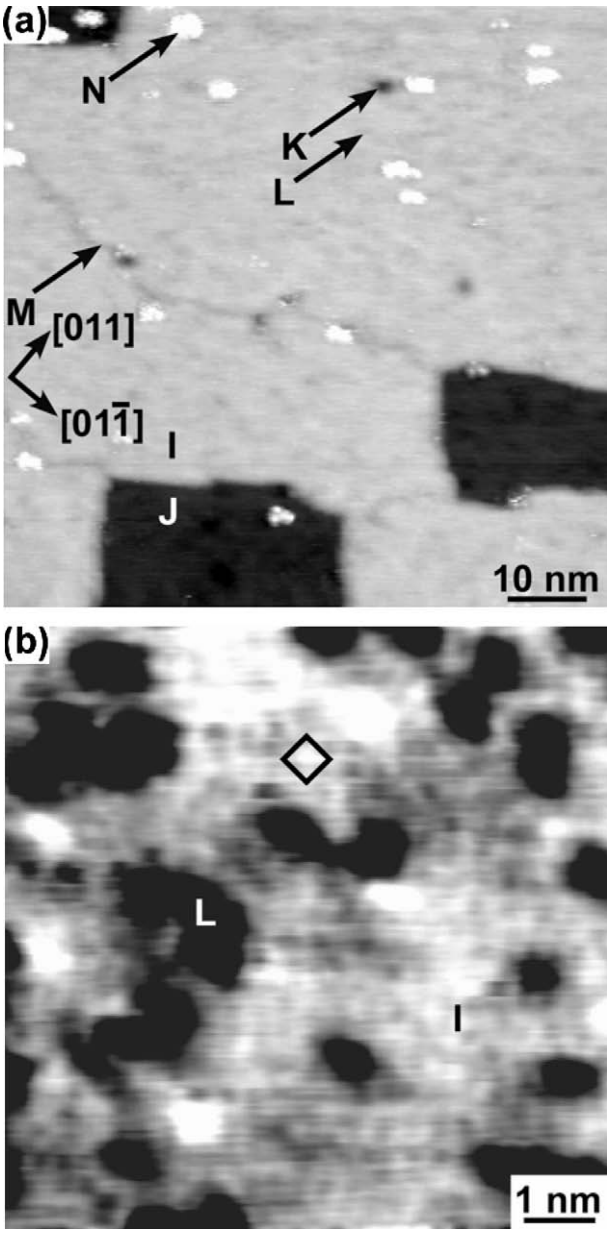

Fig. 6. STM topographs of 0.5-ML Ge/Pt(1 0 0) after annealing at 900 K. (a) Large-area scan (V_s = −0.13 V, I_t = 0.3 nA). (b) Amplified view of a mostly ordered area of (a) (V_s = −0.12 V, I_t = 0.35 nA).

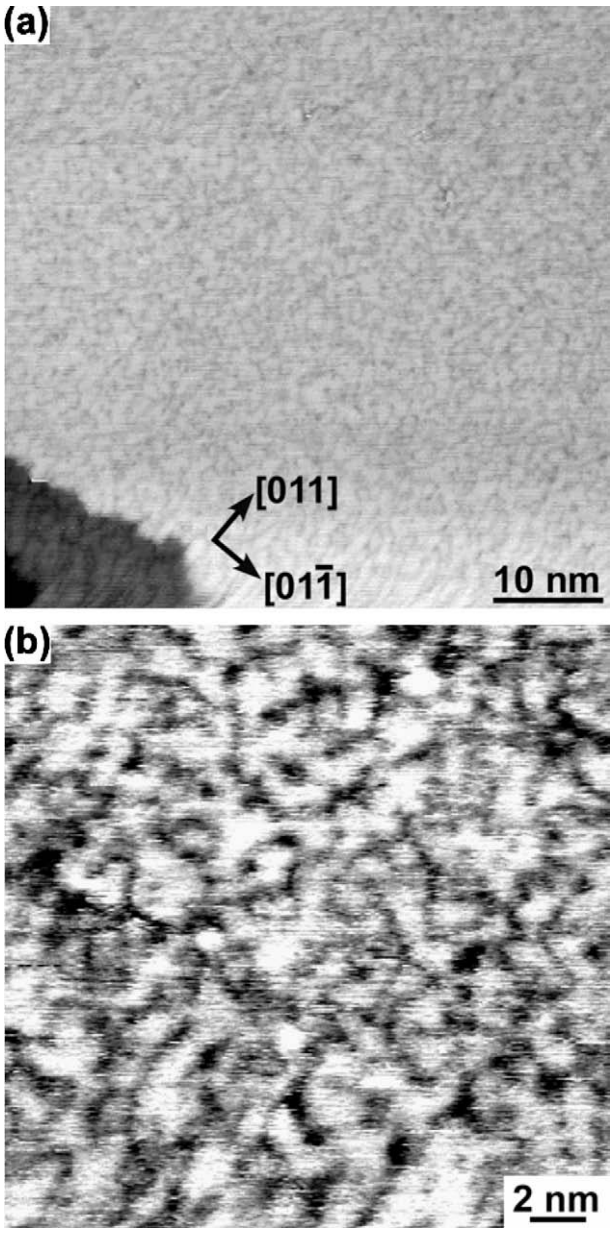

Fig. 7. STM topographs of 0.5-ML Ge/Pt(1 0 0) after annealing at 1200 K. (a) Large-area scan. (b) Amplified view of (a). V_s = −0.09 V, I_t = 0.22 nA for both images.

Wider terraces with widths of over 100 nm were observed after annealing this surface at 1200 K. This can be seen from the STM image in Fig. 7a. LEED from this surface showed only a (1 × 1)-Pt(1 0 0) pattern. XPS was used to determine that the Ge coverage was 0.13-ML. The amplified view given in Fig. 7b shows that the surface was disordered at an atomic scale. Two surface corrugations were observed as seen previously in Figs. 3, 4 and 6: Ge atoms (0.08 nm), and Pt and/or Ge-covered Pt clusters (0.15 nm). The density of bright clusters was 0.18.

3.2. CO TPD

CO adsorption was used to probe the reactivity of a c(2 × 2)-Ge/Pt(1 0 0) surface. The surface investigated was produced by deposition of 1.5-ML Ge on Pt(1 0 0) and annealing at 800 K. This surface showed a high quality c(2 × 2) LEED pattern, and excess Ge and higher temperature annealing was used to minimize the Ge vacancies and associated defects in the Ge overlayer structure. Temperature programmed desorption (TPD) curves were acquired after an exposure of 6-L CO on this c(2 × 2)-Ge/Pt(1 0 0) surface at 220 K. The result, along with a reference CO TPD trace from the (5 × 20)-Pt(1 0 0) surface, is shown in Fig. 8. As reported elsewhere [24,25], CO desorbs from the clean Pt(1 0 0) surface in a high temperature peak at 506 K. On the other hand, no CO desorption was observed from the c(2 × 2)-Ge/Pt(1 0 0) surface. This indicates that no adsorption of CO occurred on the c(2 × 2)-Ge/Pt(1 0 0) surface at 220 K.

4. Discussion

4.1. Ge deposition and lifting of the (5 × 20)-Pt(1 0 0) surface reconstruction

Deposition and growth of Ge on the (5 × 20)-Pt(1 0 0) surface at 400 K initially proceeds (after 0.2-ML Ge deposition) by the for-

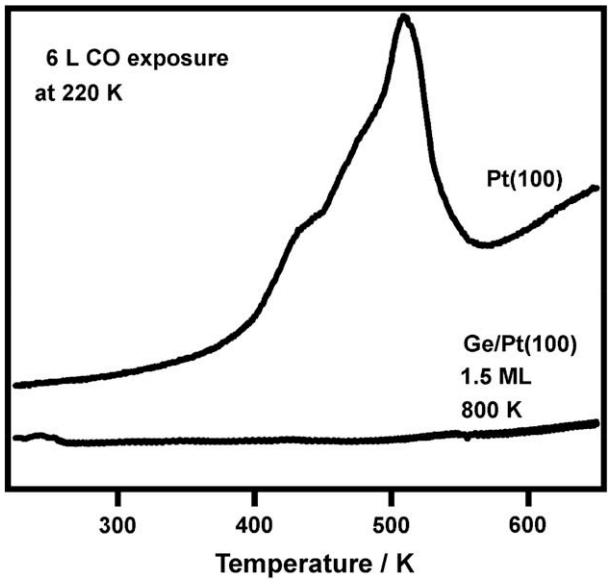

Fig. 8. CO TPD curves from the clean Pt(1 0 0) surface and c(2 × 2)-Ge/Pt(1 0 0) surface formed by deposition of 1.5-ML Ge and annealing at 850 K. CO exposures of 6-L were given on the samples at 220 K prior to heating in TPD. The heating rate was 5 K/s, and the signal for CO desorption was monitored at $m/e = 28$.

mation of elongated adislands. These adislands are considered to be comprised of deposited Ge adatoms and excess Pt atoms liberated from lifting (removing) the hex reconstruction of the clean (5 × 20)-Pt(1 0 0) surface as was observed previously for Sm [19], Au [20], and Ag [21] deposited on Pt(1 0 0). Now, we can add Ge to the list of adsorbates that interact with Pt atoms at the (5 × 20)-Pt(1 0 0) surface strongly enough and lower the surface free energy sufficiently to lift the reconstruction of the hex-surface.

4.2. c(2 × 2) structure and the directions of step edges

An ordered c(2 × 2) structure for the Ge adlayer was found as estimated by a theoretical analysis at 0.5-ML [26]. Such a structure was also produced by Sn deposition and annealing below 700 K for Sn/Pt(1 0 0) [27]. On the c(2 × 2)-Ge/Pt(1 0 0) surface, the step edges of the Ge-covered Pt substrate were along the Ge close-packed directions, as shown in Fig. 5 and described in Section 3.1.2. Likewise, on Sn/Pt(1 0 0), the step edges were along the Sn close-packed directions [27]. This direction is not stable for Pt atoms at a clean (1 × 1)-Pt(1 0 0) surface because steps form kinks due to the rotation of 45° from a Pt close-packed direction. Similar directions for step edges controlled by overlayers, away from the close-packed directions of substrate atoms, have been reported for c(4 × 2)-S/Cu(1 1 1) [28]. Adatoms of Ge and Sn with c(2 × 2) structure are considered to be adsorbed at kinks as illustrated in Fig. 9, which is proposed similarly for a c(4 × 2) S overlayer on Cu(1 1 1) [28]. A schematic model of the terraces and the step edges of a terrace, a pit (***G***) and a line vacancy of Ge (***H***), such as was observed in Fig. 5, is shown in Fig. 9.

After 0.2-ML Ge deposition and annealing at 600 K, as shown in Fig. 2, Pt islands with Ge overlayers (***A***) appear to be "round," but closer inspection shows several step edges along Ge and Pt close-packed directions. The Ge density in these domains is estimated to be only one-half of that in the c(2 × 2)-Ge overlayer. Step edges of domains with low Ge density naturally might contain both Ge and Pt close-packed directions, and are more complicated to explain than those of the uniform c(2 × 2) Ge overlayer.

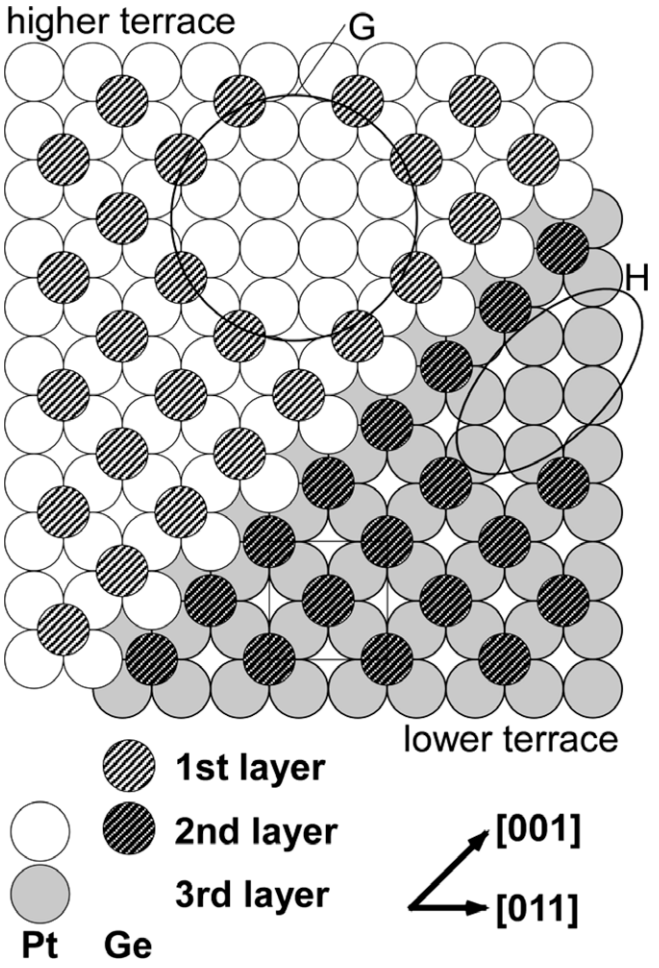

Fig. 9. Schematic model of the c(2 × 2)-Ge/Pt(1 0 0) surface. Evidence for the overlayer structure, primarily from ISS, is discussed elsewhere [29]. The superimposed square indicates the nonprimitive unit cell of the c(2 × 2) structure. Domains ***G*** and ***H*** corresponds to a pit and line vacancy formed by missing Ge adatoms, respectively, as seen in Fig. 5d.

4.3. Temperature dependence of surface structures

Increasing the temperature of the surface increases the mobility of Ge and Pt atoms at the surface. Pt atoms liberated from lifting of the hex reconstruction agglomerated in elongated islands for an "as-deposited" surface formed from 0.2-ML Ge on Pt(1 0 0) at 400 K, as shown in Fig. 1, and formed 5–40-nm wide round Pt adislands covered by Ge adatoms after annealing at 600 K as observed in Fig. 2. These adislands disappeared and only large terraces remain after annealing at 900 and 1200 K, as shown in Figs. 4 and 5. Ge adatoms were mainly in elongated islands on the "as-deposited" surface at 400 K, and then spread over 100-nm wide domains after annealing at 600 K, and then began to dissolve into the bulk of the Pt crystal after annealing at 900 and 1200 K, as confirmed by XPS [22].

After annealing at 900 and 1200 K, small adislands of Pt and/or Ge-covered Pt were observed at a density of 0.16–0.18 in disordered Ge domains in Figs. 3, 4 and 7. This density is close to 0.2, *i.e.*, that of excess Pt atoms originally packed in the (5 × 20)-Pt(1 0 0) surface layer. Therefore, these domains A and C revert to (5 × 20) upon heating to 900 K.

Ge overlayers at low coverage in Figs. 2 and 7 were revealed to be *incomplete* c(2 × 2) *structures* by ALISS [22,29], though they look disordered by STM and LEED. Only and mostly the complete c(2 × 2)

structure were observed in Figs. 5 and 6, respectively, despite vacancies of Ge adatoms. Alternate layers of the c(2 × 2) Ge layer and the (1 × 1)-Pt(1 0 0) layer could be produced by 1.5-ML Ge deposition and annealing at 600 K [22]. These congruous stabilities of c(2 × 2) Ge layers after annealing at 600–1200 K may be ascribed to repulsive interactions between Ge adatoms at nearest neighbors and attractive interactions around second-nearest neighbors.

4.4. CO adsorption

CO does not adsorb on the c(2 × 2)-Ge/Pt(1 0 0) surface at 220 K. In studies of CO adsorption on pure Ge, no CO adsorption was observed on the (2 × 8)-Ge(1 1 1) surface at 300 K [30]. Elements in Group-IV are often considered to modify transition metal surface chemistry mainly by site blocking, since they don't have valence *d* electrons that are needed to form strong bonds to CO. Two effects can be considered for the lack of CO adsorption on Ge/Pt(1 0 0). One is geometric effect. Only one-tenth of the amount of CO adsorbed on the c(2 × 2)-Sn overlayer at 310 K compared to the c(2 × 2)-Sn *surface alloy* where Sn atoms at the same coverage incorporated into the surface layer after annealing at higher temperature [31]. Sn adatoms in the overlayer strongly block access to CO adsorption sites. The other effect is due to electronic structure changes. The desorption temperature of CO decreased from 410 K on Pt(1 1 1) to 330 K on the (5 × 5)-Ge/Pt(1 1 1) *surface alloy* due to a small adsorption energy resulting from a change in the Pt electronic structure [32,33]. A similar change of electronic structure of Pt for Ge/Pt(1 0 0) surface was found by XPS as discussed elsewhere [22]. Whatever the origin, the Ge overlayer inhibited CO adsorption completely at 220 K. This suggests that Ge adatoms on a Pt surface may be useful for suppressing the deactivation of Pt catalysts by CO adsorption, which is one of the biggest problems in commercialization of fuel cells.

5. Conclusions

We have investigated the structure and morphology of surfaces formed by the deposition of Ge on a Pt(1 0 0) crystal substrate at room temperature to 400 K, along with the changes that were induced by subsequent thermal annealing. The focus in this paper is on STM and LEED observations of the initial stages of film growth following deposition of 0.2 and 0.5-ML Ge on Pt(1 0 0) and the formation of an ordered c(2 × 2) structure at the surface. Another paper reports on Na^+-ISS, XPS, and XPD data, including results for larger Ge depositions, which enables the assignment of the c(2 × 2) structure to an ordered Ge adlayer [22].

In the initial stages of film growth, deposition of 0.2-ML Ge on Pt(1 0 0) at 400 K formed elongated islands comprised of intermixed Ge atoms and Pt that was ejected from the first layer by lifting of the hex or (5 × 20) reconstruction of the clean Pt(1 0 0) surface. Annealing this Ge/Pt(1 0 0) surface at 600 K dispersed Ge atoms to form continuous disordered Ge overlayers spread over 100-nm wide domains. "Round" Pt islands were produced from the excess Pt atoms that were expelled into the Ge adlayer and stabilized under Ge adlayers.

Deposition of 0.5-ML Ge on Pt(1 0 0) at room temperature and annealing this surface at 600 K produced a c(2 × 2) structure, assigned to a c(2 × 2)-Ge adlayer that was characterized by STM and LEED. Defects in this structure arose from square and rectangular Ge vacancies that were up to several nanometers across, but apparently not from disordered Ge adatoms. Thus, the c(2 × 2) structure is more stable than disordered Ge domains for Ge overlayers around 0.5-ML. The step edges of the c(2 × 2)-Ge adlayer islands are different from that of the Pt(1 0 0) surface by 45°, but occur along the close-packed direction of Ge adatoms in the c(2 × 2) structure. This has the effect of stabilizing the kinks of Pt terraces by adsorption of Ge. Though annealing this surface to 900 K resulted in more Ge vacancies, the c(2 × 2) structure domain was observed by STM and the LEED pattern showed the c(2 × 2) structure. Ge adatoms still remained on the Pt(1 0 0) surface to very high temperatures, even after heating surfaces containing 0.2-ML Ge on Pt(1 0 0) to either 900 or 1200 K, and annealing surfaces with 0.5-ML Ge on Pt(100) to 1200 K. These domains looked disordered by STM, while ISS results indicate they are ordered locally but incomplete as discussed elsewhere [22]. It was found that the c(2 × 2) Ge overlayers are preferentially produced on Pt(1 0 0).

TPD results showed CO chemisorption was completely inhibited on a Pt(1 0 0) surface by the c(2 × 2) Ge overlayer at 220 K. This suggested that the chemistry and catalysis of such Ge/Pt(1 0 0) surfaces will be strongly altered due to site blocking and Pt electronic structure changes.

Acknowledgement

This work was partially supported by the Analytical and Surface Chemistry Program in the Division of Chemistry, National Science Foundation.

References

[1] M.G. Grimaldi, L. Wielunski, M.-A. Nicolet, Thin Solid Films 81 (1981) 207. and references therein.
[2] Y.F. Hsieh, L.J. Chen, Journal of Applied Physics 63 (1988) 1177. and references therein.
[3] T. Komatsu, M. Mesuda, T. Yashima, Applied Catalysis A 194–195 (2000) 333.
[4] T. Komatsu, S. Hyodo, T. Yashima, Journal of Physical Chemistry B 101 (1997) 5565.
[5] S.R. Miguel, M.C. Roman-Martnez, D. Cazorla-Amoros, E.L. Jablonski, O.A. Scelza, Catalysis Today 66 (2001) 289.
[6] A. Borgna, T.F. Garetto, C.R. Apesteguía, B. Moraweck, Applied Catalysis A 182 (1999) 189.
[7] S. Motoo, M. Watanabe, Journal of Electroanalytical Chemistry 69 (1976) 429.
[8] N. Furuya, S. Motoo, Journal of Electroanalytical Chemistry 98 (1979) 195.
[9] R. Lbibb, R. Castanet, Journal of Alloys and Compounds 189 (1992) 23.
[10] F.R. der Boer, R. Boom, W.C.M. Mattens, A.R. Miedema, A.K. Niessen, Cohesion in Metals, Elsevier Science Publishers, Amsterdam, 1988.
[11] C. Ho, S. Banerjee, M. Batzill, C.E. Beck, B.E. Koel, Surface Science 603 (2009) 1161.
[12] K. Fukutani, Y. Murata, J. Brillo, H. Kuhlenbek, H.-J. Freund, M. Taguchi, Surface Science 464 (2000) 48.
[13] W. Chen, L. Severin, M. Göster, M. Hammer, S. Cameron, J. Paul, Physical Review B 50 (1994) 5620.
[14] D.E. Eastman, F.J. Himpsel, J.F. van der Veen, Journal of Vacuum Science and Technology 20 (1982) 609.
[15] K. Terakura, Journal of Physics F 7 (1977) 1773.
[16] G. Ritz, M. Schmid, P. Varga, A. Borg, M. Rønning, Physical Review B 56 (1997) 10518.
[17] S. Hagstrum, H.B. Lyon, G. Somorjai, Physical Review Letters 15 (1965) 491.
[18] Y.Y. Yeo, C.E. Wartnaby, D.A. King, Science 268 (1995) 1731.
[19] H.J. Venvik, C. Berg, A. Borg, S. Raan, Physical Review B 53 (1996) 16587.
[20] C. Berg, H.J. Venvik, F. Strisland, A. Ramstad, A. Borg, Surface Science 409 (1998) 1.
[21] M. Batzill, B.E. Koel, Surface Science 498 (2002) L85.
[22] T. Matsumoto, C. Ho, M. Batzill, B.E. Koel, Physical Review B, submitted for publication.
[23] D. Beck, M. Batzill, C. Baur, K. Jooho, B.E. Koel, Review of Scientific Instruments 73 (2002) 1267.
[24] M.A. Barteau, E.I. Ko, R.J. Madix, Surface Science 102 (1981) 99.
[25] T. Matsumoto, M. Batzill, S. Hsieh, B.E. Koel, Surface Science 572 (2004) 146.
[26] G. He, Physical Review B 71 (2005) 195409.
[27] M. Batzill, D. Beck, B.E. Koel, Surface Science 558 (2004) 35.
[28] S. Rousset, S. Gauthier, O. Siboulet, W. Sacks, M. Belin, J. Klein, Journal of Vacuum Science and Technology A 8 (1989) 302.
[29] M. Batzill, T. Matsumoto, C. Ho, B.E. Koel, Physical Review B 69 (2004) R113401.
[30] T. Sakurai, H.D. Hagstrum, Physical Review B 20 (1979) 2423.
[31] Y. Li, B.E. Koel, Surface Science 330 (1995) 193.
[32] K. Fukutani, T.T. Mogkoev, Y. Murata, K. Terakura, Surface Science 363 (1996) 185.
[33] K. Fukutani, T.T. Mogkoev, Y. Murata, M. Matsumoto, T. Kawauchi, T. Magome, Y. Tezuka, S. Shin, Journal of Electron Spectroscopy and Related Phenomena 88–91 (1998) 597.